Frontiers in Bioscience Landmark

Front. Biosci. (Landmark Ed) **2024**; 29(1): 35
https://doi.org/10.31083/j.fbl2901035

Original Research

Downregulation of MTHFD2 Inhibits Proliferation and Enhances Chemosensitivity in Hepatocellular Carcinoma via PI3K/AKT Pathway

Jie Wang[1,†], Ze Yu[1,†], Yixiao Jiang[2], Ting Le[1], Yixin Wu[1], Ziqi Li[1], Guoqiang Zhang[2], Feiyue Wu[3,*], Haijie Ma[1,*]

[1]Cellular and Molecular Biology Laboratory, Zhoushan Hospital, Wenzhou Medical University, 316021 Zhoushan, Zhejiang, China
[2]Department of General Surgery, Zhoushan Hospital, 316021 Zhoushan, Zhejiang, China
[3]Department of Pharmacy, Zhoushan Hospital, 316021 Zhoushan, Zhejiang, China
*Correspondence: zswufeiyue@163.com (Feiyue Wu); haijie215@163.com (Haijie Ma)
[†]These authors contributed equally.

Academic Editor: Alfonso Urbanucci
Submitted: 26 September 2023 Revised: 3 November 2023 Accepted: 27 November 2023 Published: 19 January 2024

Abstract

Background: Despite the substantial impact of methylenetetrahydrofolate dehydrogenase 2 (MTHFD2) on cancer progression, its significance in the regulation of hepatocellular carcinoma (HCC) cell proliferation and chemosensitivity remains poorly defined. **Methods**: We evaluated MTHFD2 expression in a total of 95 HCC tissues by immunohistochemistry and analyzed the association of MTHFD2 with clinicopathologic features. qRT-PCR and Western blotting were conducted to verify MTHFD2 expression levels. Bioinformatics analysis such as gene set enrichment analysis (GSEA) and kyoto encyclopedia of genes and genomes (KEGG) enrichment analysis were used to predict the signaling pathways involved in MTHFD2. In addition, to investigate the anti-tumor effects of MTHFD2 knockdown, Cell Counting Kit-8 (CCK-8) and EdU assays were used. **Results**: We found that MTHFD2 was frequently upregulated in HCC, and the combination of increased expression of MTHFD2 and Ki67 was associated with poor HCC prognosis. MTHFD2 knockdown significantly inhibited HCC cell proliferation and effectively sensitized HCC cells to sorafenib and lenvatinib. PI3K/AKT pathway was involved in MTHFD2-mediated modulation of proliferation and chemosensitivity. **Conclusions**: These findings indicate that MTHFD2 plays an important role in proliferation and chemosensitivity of HCC, indicating that it may serve as a novel pharmacological target for improving HCC therapy.

Keywords: MTHFD2; proliferation; chemosensitivity; HCC; Ki-67

1. Introduction

Hepatocellular carcinoma (HCC) poses a major health problem worldwide as it ranks as the sixth most prevalent tumor and the third-leading cause of cancer-related deaths [1,2]. Despite improvements in surgical methods and systemic chemotherapy, the long-term survival rate for patients with HCC still remains unsatisfactory [3,4]. Hence, it is imperative to identify the mechanisms contributing to HCC progression and chemoresistance.

Accumulating evidence has indicated that tumor cells often rewire their metabolic signaling pathways for adaption to nutrient stress and/or promote cancer cell proliferation [5,6], such as folate-mediated one-carbon metabolism (FOCM) [7]. In the folate cycle, the transfer of a single carbon unit from tetrahydrofolate to downstream acceptors in the mitochondrial and cytoplasmic compartments is linked with the three major metabolic cycles of the liver [8,9]. The distinctive single-carbon pathway generates necessary metabolites for cellular development, including nucleotides and the nicotinamide adenine dinucleotide phosphate hydrogen (NADPH) [10,11]. Therefore, a detailed analysis aimed at understanding the molecular mechanism of folate cycle metabolism may provide key insight into developing novel therapeutic strategies.

Methylenetetrahydrofolate dehydrogenase 2 (MTHFD2), a key formyltetrahydrofolate synthetase and cyclohydrolase enzyme, efficiently drives the folate cycle in embryonic tissue to support growth and proliferation [12]. Interestingly, MTHFD2 is also upregulated in several tumors to promote cancer cell proliferation and tumor progression by meeting the high demands for amino acid and nucleotide biosynthesis [13], while its expression is negligible in most healthy adult tissues [14]. Given this expression pattern, MTHFD2 has attracted much attention in cancer research. However, the functions of MTHFD2 in the regulation of HCC proliferation and chemosensitivity remain unclear.

In the present study, we found that MTHFD2 was frequently upregulated in HCC tissues, and combining its high expression with high Ki67 was correlated with the poor HCC prognosis. Furthermore, downregulation of MTHFD2 significantly inhibited cell proliferation and effectively sensitized HCC cells to sorafenib and lenvatinib by downregulating PI3K/AKT signaling. Our study strongly highlights the significance of MTHFD2 in HCC cell proliferation and chemosensitivity and therefore provides a potential strategy for improving HCC treatment strategies.

2. Materials and Methods

2.1 Chemicals and Reagents

Chemicals and reagents were acquired from designated suppliers: SC79 (Cat No. T2274; TargetMol, Shanghai, China), DMSO (Cat No. D4540; Sigma-Aldrich, Darmstadt, Germany), Sorafenib (Cat No. HY-10201; MCE, Monmouth Junction, NJ, USA), Lenvatinib (Cat No. HY-10981; MCE, Monmouth Junction, NJ, USA), LY345899 (Cat No. T15827; TargetMol, Shanghai, China), FBS (Cat. No. 10099141C; Gibco, Grand Island, NY, USA), Lipofectamine RNAiMAX Transfection Reagent (Cat No. 13778500; Thermo Fisher Scientific, Waltham, MA, USA), CCK-8 Kit (Cat No. C008; 7Sea, Shanghai, China), Detergent Compatible Bradford Protein Assay Kit (Cat No.P0006C; Beyotime, Hangzhou, China), MycoBlue Mycoplasma Detector (Cat No. D101-01; Vazyme, Nanjing, China), Cell-Light EdU In Vitro Kit (Cat No. C10310; RiboBio, Guangzhou, China), TRIzol reagent (Cat No. 15596026; Thermo Fisher Scientific, Waltham, MA, USA), SYBR Premix Ex Taq Kit (Cat No. AKA1105; TaKaRa, Tokyo, Japan), PrimeScript II 1st Strand cDNA Synthesis Kit (Cat No. 6210A; TaKaRa, Tokyo, Japan), 1X SDS-PAGE Sample Loading Buffer (Cat No. P0015A; Beyotime, Hangzhou, China), SuperSignal West Femto (Cat No. 34094; Thermo Fisher Scientific, Waltham, MA, USA), BSA (Cat No. 4240GR500; Saiguo, Guangzhou, China).

Antibodies were obtained from the following sources: p-AKT (Ser473) (1:1000, Cat No. 4060; CST, Danvers, MA, USA), AKT (1:1000, Cat No. 4691; CST, Danvers, MA, USA), MTHFD2 (1:1000, Cat. No. H00010797-M01; Abnova, Taipei, China), Ki-67 (1:500, Cat No. ET1609-34; HUABIO, Hangzhou, China), and β-actin (1:3000, Cat No. A5441; Sigma-Aldrich, Darmstadt, Germany).

2.2 Patients and Samples

The HCC tissue microarray (Cat No. HLiv-HCC180Sur-05) was obtained from Outdo BioTech (Shanghai, China). The HLiv-HCC180Sur-05 contained 95 HCC tissues and 85 adjacent tissues, 85 of which were paired tissues. Detailed clinicopathological features of the cohorts were also provided by Outdo BioTech (Shanghai, China). And other 35 pairs of matched HCC tissue samples were obtained from Zhoushan Hospitital (Zhoushan, China). An Ethics Committee approved by the appropriate hospital obtained written informed consent from each subject or subject's guardian.

2.3 Immunohistochemistry (IHC) and Scoring

Tumor tissues and adjacent normal tissues were fixed with 10% neutral formalin for a duration of 48 h, following standard procedures for paraffin embedding. Subsequently, the tissues were sliced into sections measuring 4 µm. The tissue sections were then subjected to treatment with 1 mM EDTA (pH = 8.0) and 3% H_2O_2 for a duration of 10 min. Following antigen retrieval using citrate buffer (pH = 6.0), the sections were blocked with 1% BSA for 30 min and subsequently incubated with anti-MTHFD2 antibody and anti-Ki-67 antibody at a temperature of 4 °C overnight. The immunostaining procedure employed the streptavidin-biotin peroxidase complex method (K060911, Dako). After rinsing in PBS, the peroxidase reaction was visualized through incubation with 3, 3′-Diaminobenzidine tetrahydrochloride (DAB). The results were assessed by grading the proportion of MTHFD2 positively stained cells was graded as follows: less than 5%–grade 0; 5% to 25%–grade 1; 26% to 50%–grade 2; 51% to 75%–grade 3; more than 75%–grade 4. The staining grades were categorized as follows: 0 denoted no staining; 1 indicated weakly positive staining; 2 represented medium staining; 3 denoted strong staining. Based on the sum of the two results: a total score of 0–1 indicated no staining (–), 2–3 denoted weakly positive (+), 4–5 represented medium positive (++), and 6–7 indicated strongly positive (+++). Additionally, the combination of (–, +) was considered as low expression, while (++, +++) indicated high expression [15]. The Ki-67 labeling index (LI) was evaluated by determining the percentage of cells exhibiting positively staining. With the threshold value of 10%, HCC lesions were categorized into the low Ki-67 group (Ki-67 LI $\leq$10%) and the high Ki-67 group (Ki-67 LI $>$10%) [16]. The quantification of positively stained cells was performed by two pathologists independently, following a blinded manner, and a consensus was reached to establish the final outcome.

2.4 Cell Culture and Transfection

The human HCC cell lines, SMMC-7721 and HepG2, were obtained from the National Collection of Authenticated Cell Cultures. Cells were cultured in Dulbecco's Modified Eagle Medium (DMEM) supplemented with 10% fetal bovine serum (FBS) at 37 °C in a humidified atmosphere of 5% CO_2 in an incubator. All cell lines were validated by STR profiling and tested negative for mycoplasma (MycoBlue Mycoplasma Detection Kit). The transfection of siRNA was carried out utilizing the Lipofectamine™ RNAiMAX Transfection Reagent. All experimental procedures were performed according to the manufacturer's protocols.

2.5 RNA Interference

In accordance with the manufacturer's protocol, the cells were transfected with 100 nM of siRNAs targeting MTHFD2 or the control. The target sequences of siRNAs were shown in the **Supplementary Material**.

2.6 Real-Time Quantity PCR

A quantity of 5 µg of RNA was extracted from HCC tumor tissues and matched adjacent tissues using TRIzol reagent. Subsequently, the entire RNA was transcribed into cDNA using the PrimeScript II 1st Strand cDNA Synthesis Kit. The SYBR Premix Ex Taq Kit was employed for

conducting quantitative PCR with the Applied Biosystems 7500 Real-Time PCR System (Applied Biosystems, Hammonton, NJ, USA). The relative expression was obtained using the $2^{-\triangle\triangle Ct}$ method by using *GAPDH* as the reference gene. The primer sequences of *MTHFD2* and *GAPDH* were shown in **Supplementary Material**.

2.7 Western Blotting

Cells were washed twice using ice-cold PBS, and protein extracts were prepared using RIPA reagent. The concentration was quantified using the Bradford assay. Subsequently, 30 µg of proteins were subjected to SDS-PAGE and transferred onto PVDF membranes. Protein analysis was conducted using antibodies against MTHFD2, p-AKT (Ser473), AKT, and β-actin were used for protein analysis. Bands were identified using enhanced chemiluminescence.

2.8 Cell Proliferation Assay

A total of 3×10^3 cells were seeded onto 96-well plates before experiments. After incubating at 37 °C for 24 h, cells were treated with sorafenib or lenvatinib for 72 h. Cell proliferation activity was conducted using the CCK-8 Kit. Specifically, 10 µL of cell counting solution was added to each well, followed by an incubation at 37 °C for 2 h. Subsequently, the absorbance of the solution was measured at a wavelength of 450 nm.

2.9 EdU Assay

The EdU proliferation test was performed according to the manufacturer's protocol. After incubation at 37 °C, cells were added with 50 µM EdU and incubated for 2 h. Cells were then treated with 4% paraformaldehyde and then subjected to staining using Apollo Dye Solution. Nucleus was stained with hoechst33342. The images were taken using Leica Application Suite (version 3.0.0, Leica Microsystems, Wetzlar, Germany).

2.10 Bioinformatics Analysis

The bioinformatics analysis software and website were presented in the **Supplementary Material**.

2.11 Statistical Analysis

All data were analyzed with GraphPad Prism 6.0 (GraphPad Software, Inc., San Diego, CA, USA). The bar graphs depict the fold changes or percentage relative to the control, along with a standard deviation of three independent experiments. Student's *t*-test was employed for the analysis of normally distributed data, while one-way ANOVA with Tukey's multiple comparisons was utilized for the analysis of more than two groups. Survival was estimated by the Kaplan–Meier method and compared by the log-rank test. Statistical significance was determined as a p value below 0.05. Levels of significance were denoted as $*p < 0.05$, $**p < 0.01$, $***p < 0.001$, $****p < 0.0001$.

3. Results

3.1 Expression Analysis of Genes Related to Folate Metabolism in Liver Cancer

To investigate the role of folate metabolism-related genes in liver cancer, we first analyzed the changes in mRNA expression profiles and kyoto encyclopedia of genes and genomes (KEGG)/gene ontology (GO) pathways using the gene expression omnibus (GEO) database (GSE112790) (Fig. 1A; **Supplementary Fig. 1**). Then, we focused our initial efforts on 5 differentially-expressed genes (DEGs) with overlapping functions with folate metabolism-related genes (Fig. 1B). Of these, two genes (*TYMS* and *MTHFD2*) were upregulated and three genes (*ALDH1L1*, *MTHFD2L*, and *FTCD*) were reduced in HCC tumors relative to normal liver tissue (Fig. 1C,D).

Next, we performed LASSO regression analysis for the 5 genes related to folate metabolism to establish a prognostic model (Fig. 1E). Specifically, the model is a RiskScore formula containing multiple genes where each gene is assigned a numeric weight, a negative number represents a protective gene (*FTCD*), and the positive number represents risk genes (*TYMS*, *MTHFD2*, *ALDH1L1*, and *MTHFD2L*). The calculated Riskscore = (0.0129) $\times$ MTHFD2 + (–0.146) $\times$ FTCD + (0.0449) $\times$ ALDH1L1 + (0.1948) $\times$ MTHFD2L + (0.1475) $\times$ TYMS.

These 5 DEGs were subsequently used to divided HCC patients into high-risk and low-risk groups (Fig. 2A). Their survival status is shown in Fig. 2B. There was a highly significant difference in survival between the high and low-risk groups ($p = 1.86 \times 10^{-5}$). Prognostic survival prediction was performed at 1, 3, and 5 year intervals, and a prognostic model, specifically ROC-AUC score for 1 year, showed a notable separability (Fig. 2C).

3.2 MTHFD2 is Upregulated in HCC

MTHFD2 is a key enzyme in the folate-mediated metabolism pathway that is often hyperactivated in human cancers [17–19]. Thus, we examined its expression in 35 pairs of matched HCC/normal tissue samples using qRT-PCR. As shown in Fig. 2D, MTHFD2 mRNA abundance was significantly higher in HCC tissues compared with their adjacent counterparts in 18 out of 35 (51.4%) cases ($p < 0.01$). In addition, IHC analysis of 85 pairs of patient-matched HCC/normal tissue samples included in a HCC tissue microarray indicated that higher staining intensity was observed in 63 (74.1%) of HCC tissues compared to matched normal tissues (Fig. 2E). The expression of MTHFD2 was positively related to histologic grade and Ki-67 expression through clinic-pathological correlation analysis. Here we also noted a significant ($p < 0.0001$) correlation between the expression of Ki-67 and histologic grade (Table 1). Thus, data obtained indicate that MTHFD2 is overexpressed in HCC tissues and potentially involved in disease progression.

Ki-67 is a traditional proliferation marker widely used in studies of various cancer types, including HCC. Further-

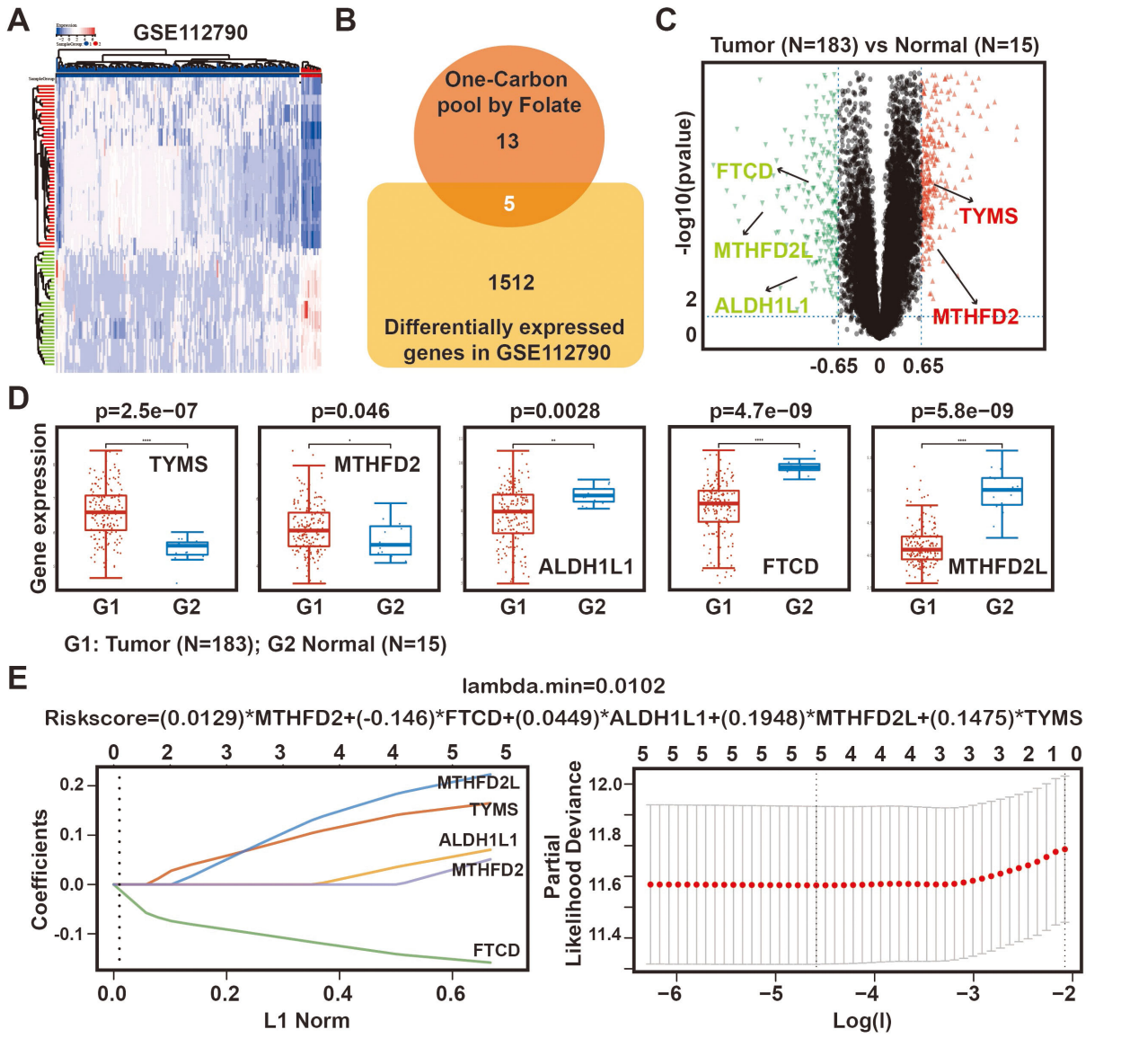

Fig. 1. Analysis of folate metabolism-related genes in liver cancer. (A) Heat map of differentially expressed mRNAs in GEO112790. (B) Venn diagram of the differentially expressed genes (DEGs) in GSE112790 and genes associated with the folate cycle (C) Volcano plots of the DEGs. (D) Differential expression analysis of five genes in GSE112790. (E) The LASSO partial likelihood deviance plot and the coefficient profiles of these 5 genes. *$p < 0.05$, **$p < 0.01$, ****$p < 0.0001$.

more, tumor histologic grade has also been found to be tightly associated with tumor prognosis [20,21]. Consequently, we examined the influence of MTHFD2 and Ki-67 expression on the survival of patients using Kaplan-Meier analysis with the long-rank test. Findings obtained indicated that the poorer overall survival was associated with the combination of high MTHFD2 and high Ki-67 levels ($p < 0.05$), while the expression of MTHFD2 or Ki-67 alone showed no statistically significant difference in HCC patient survival (Fig. 2F). These findings suggest MTHFD2 is a potential prognostic biomarker for HCC.

3.3 Downregulation of MTHFD2 Inhibits HCC Cell Proliferation

Next, we explored the biological significance of MTHFD2 expression on various signaling pathways using gene set enrichment analysis (GSEA) analysis, and found that comparing the MTHFD2-high versus the MTHFD2-low groups indicated a significantly enrichment in multiple proliferation-related pathways. It is generally believed that the $|NES| > 1$, $p < 0.05$ pathway is significantly enriched. As shown in our GSEA analysis (Fig. 3A), compared with the MTHFD2-low expression group, the MTHFD2-high group was significantly associated with the proliferation-related pathways, including VEGF signaling, ERBB signaling and cell adhesion.

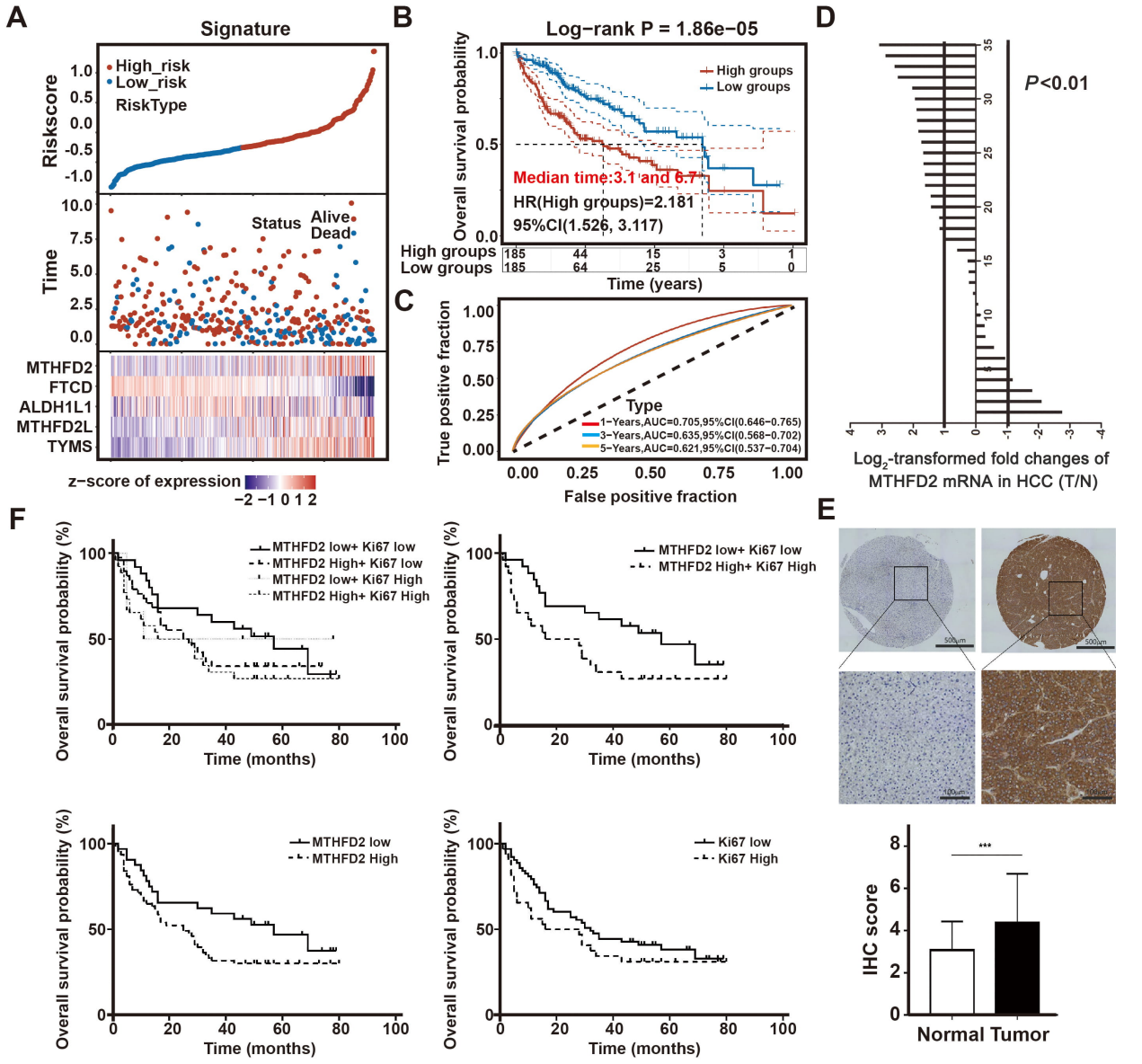

Fig. 2. MTHFD2 is overexpressed in hepatocellular carcinoma (HCC) tissues. (A) Distribution of risk scores for the 5-genes model. (B) Kaplan-Meier survival curve of the patients in the high-risk and low-risk groups for OS. (C) Time-related ROC analysis proved the prognostic performance of the risk score in the training set. (D) The methylenetetrahydrofolate dehydrogenase 2 (MTHFD2) mRNA expression between tumor and normal tissues was detected by qRT-PCR (n = 35). (E) Immunohistochemical staining images of the tumor and normal tissues. (F) Kaplan-Meier analysis according to different combinations of MTHFD2 and Ki67 expression. ***$p <$ 0.001. ROC, receiver operating characteristic; OS, overall survival; qRT-PCR, quantitative real-time reverse transcription polymerase chain reaction.

Therefore, to evaluate the effect of MTHFD2 on HCC cell proliferation, MTHFD2 was knocked down in SMMC-7721 and HepG2 HCC cell lines (Fig. 3B). As shown in Fig. 3C,D, knockdown of MTHFD2 considerably decreased cell proliferation ability, suggesting a significant role in modulating HCC cell activity. Additionally, the MTHFD2 inhibitor LY345899 also reduced the proliferation of HCC (**Supplementary Fig. 3**).

3.4 MTHFD2 Regulates HCC Cell Proliferation through the PI3K/AKT Signaling Pathway

To investigate the mechanism underlying the effect of MTHFD2 on cell proliferation, bioinformatic analysis was utilized to analyze the correlation between signaling pathways and MTHFD2 expression. Firstly, the expression profile data and corresponding clinical information from liver cancer patients in the cancer genome atlas (TCGA) dataset were downloaded. Second, bioinformatic analysis was applied and results show that PI3K/AKT signaling is the most enriched pathway associated with MTHFD2 ex-

Table 1. Association between MTHFD2/Ki67 expression and characteristics of patients.

Group	Overall (n = 95)	MTHFD2 expression		*p* value	Ki-67 expression		*p* value
		Low (n = 32)	High (n = 63)		Low (n = 63)	High (n = 32)	
Age (years)				0.337			0.066
≤55	54 (56.8)	16 (50.0)	38 (60.3)		40 (63.5)	14 (43.8)	
>55	41 (43.2)	16 (50.0)	25 (39.7)		23 (36.5)	18 (56.2)	
Gender				0.794			0.333
Male	85 (89.5)	29 (90.6)	56 (88.9)		55 (87.3)	30 (93.7)	
Female	10 (10.5)	3 (9.4)	7 (11.1)		8 (12.7)	2 (6.3)	
Tumor size (cm)				0.517			0.509
≤5	43 (45.3)	13 (40.6)	30 (47.6)		27 (42.9)	16 (50.0)	
>5	52 (54.7)	19 (59.4)	33 (52.4)		36 (57.1)	16 (50.0)	
Liver cirrhosis				0.162			0.696
Without	59 (62.1)	23 (71.9)	36 (57.1)		40 (63.5)	19 (59.4)	
With	36 (37.9)	9 (28.1)	27 (42.9)		23 (36.5)	13 (40.6)	
Portal vein invasion				0.594			0.594
Without	88 (92.6)	29 (90.6)	59 (93.7)		59 (93.7)	29 (90.6)	
With	7 (7.4)	3 (9.4)	4 (6.3)		4 (6.3)	3 (9.4)	
Histologic grade				0.040			<0.0001
G1	3 (3.2)	0 (0.0)	3 (4.8)		3 (4.8)	0 (0.0)	
G2	58 (61.0)	25 (78.1)	33 (52.3)		47 (74.6)	11 (34.4)	
G3	34 (35.8)	7 (21.9)	27 (42.9)		13 (20.6)	21 (65.6)	
TNM				0.826			0.516
I&II	46 (48,4)	16 (50.0)	30 (47.6)		32 (50.8)	14 (43.8)	
III&VI	49 (51.6)	16 (50.0)	33 (52.4)		31 (49.2)	18 (56.2)	
Metastasis				0.308			0.622
Without	93 (97.9)	32 (100.0)	61 (96.8)		62 (98.4)	31 (96.9)	
With	2 (2.1)	0 (0.0)	2 (3.2)		1 (1.6)	1 (3.1)	
Survival				0.108			0.511
Deceased	61 (64.2)	17 (53.1)	44 (69.8)		39 (61.9)	22 (68.7)	
Alive	34 (35.8)	15 (46.9)	19 (30.2)		24 (38.1)	10 (31.3)	
Ki-67				0.028			
≤10%	63 (66.3)	26 (81.3)	37 (58.7)				
>10%	32 (33.7)	6 (18.7)	26 (41.3)				

TNM, tumor node metastasis.

pression with 90 up-regulated genes participating in this signaling axis, and its GeneRatio score is the highest among all signals (Fig. 4A,B; **Supplementary Fig. 2**).

The correlations between MTHFD2 and pathway scores were examined using Spearman analysis. We selected four pathways that were significantly correlated with tumor malignancy and analyzed their correlation with MTHFD2 expression. Results indicated that all four pathways showed a significant positive correlation with MTHFD2 ($r > 0$), and the PI3K/AKT signaling axis displayed the most significant correlation with MTHFD2 expression ($r = 0.61$) (Fig. 4C). As shown in Fig. 4D, the levels of AKT phosphorylation at Ser473 in MTHFD2-silenced HCC cells were significantly lower than those in siRNA control cells. By incubating HCC cells with the novel AKT activator SC79, inhibitory effects on proliferation displayed by MTHFD2 knockdown or inhibited cells were notably reversed (Fig. 4E–G). Thus, knockdown of MTHFD2 suppresses cell growth signaling mediated by PI3K/AKT signaling in HCC cells.

3.5 Knockdown of MTHFD2 Sensitizes HCC Cells to Sorafenib and Lenvatinib

To confirm whether MTHFD2 expression impacts HCC cell chemosensitivity, MTHFD2 was knocked down in SMMC-7721 and HepG2 cell lines followed by treatment with sorafenib or lenvatinib. As shown in Fig. 5 and **Supplementary Fig. 4**, MTHFD2 knockdown resulted in decreased proliferative ability compared with control groups, indicating that knockdown of MTHFD2 effectively sensitizes HCC cells to sorafenib and lenvatinib.

4. Discussion

Accumulating evidence indicates the combination of Ki-67 and other molecular markers can be used to more accurately predict patient prognosis in various cancers [22–26]. In this study, the heightened expression of MTHFD2 is positively associated with increased Ki-67 expression in HCC. Moreover, combining MTHFD2 with Ki-67 notably predicted poorer prognosis for HCC patients, while either

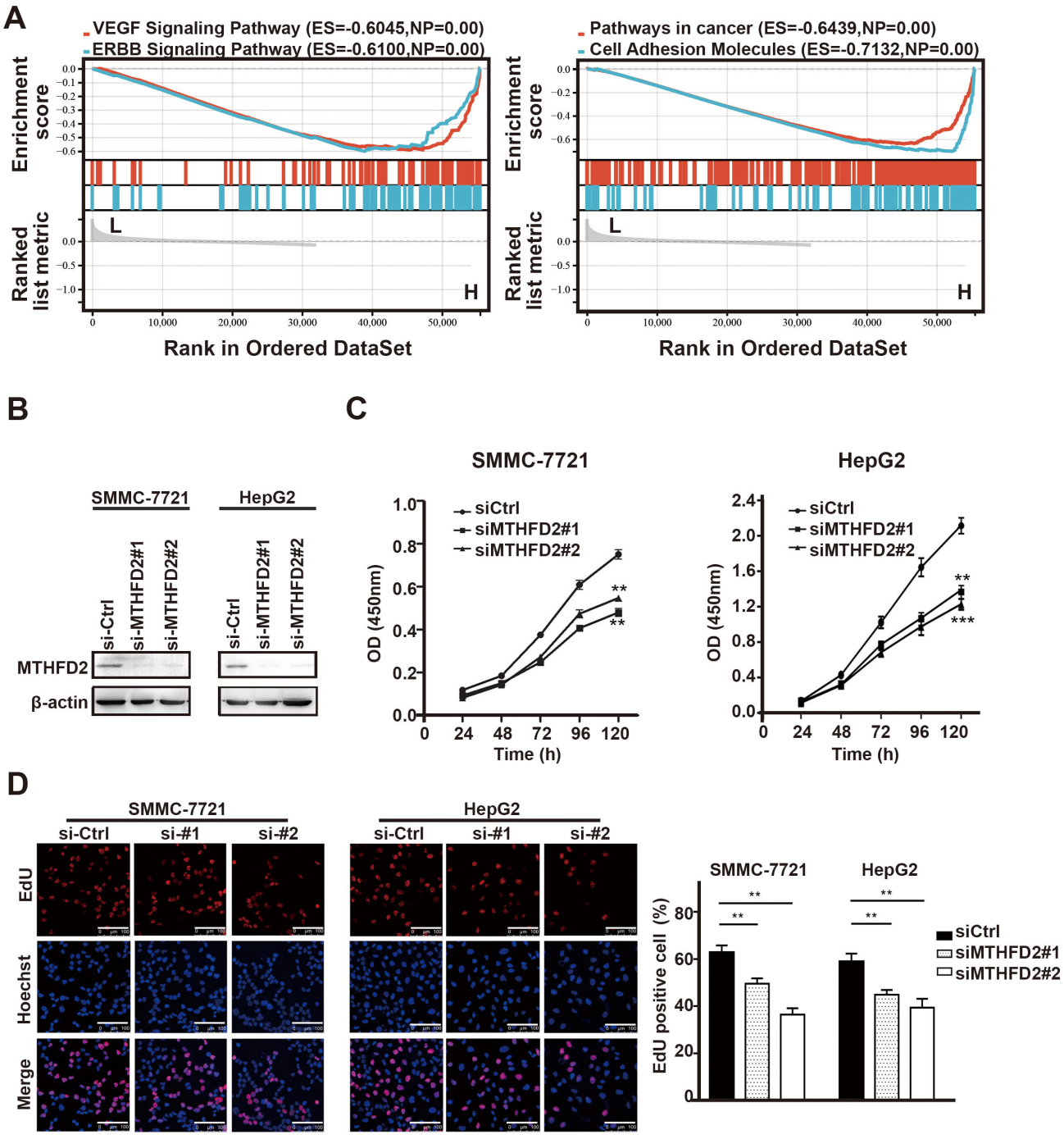

Fig. 3. Downregulation of MTHFD2 inhibits the proliferation of HCC. (A) Gene set enrichment analysis (GSEA) showed that several Proliferation-related signal pathways were inhibited in the MTHFD2-low group. (B) Western blotting analysis showed the MTHFD2 knockdown efficiency with two unique siRNAs (#1, #2) in SMMC-7721 and HepG2 cells. (C) Effects of MTHFD2 knockdown on cell proliferation were assessed by CCK-8 cell proliferation assay. (D) DNA synthesis in SMMC-7721 and HepG2 cells was measured using the EdU assay. Photographs were taken under an optical microscope with a magnification of 400×. Experiments were performed three times independently and the data were represented as the means ± SD. $^{**}p < 0.01$, $^{***}p < 0.001$.

MTHFD2 or Ki-67 alone showed no significant impact on HCC patient overall survival, suggesting the clinical value in diagnosing HCC. However, due to small overall sample sizes for HCC patients, analyses such as Cox regression may be affected by bias; thus, further validation are required.

Several studies have suggested that mitochondrial FOCM, which is highly correlated with cancer malignancy [27], acts as a critical regulator of NAD(P)H, ATP, glycine, and one-carbon unit biosynthesis used for cytoplasmic biosynthetic reactions [11,28]. For example, serine hydroxymethyltransferase-2 (SHMT2) over-expression

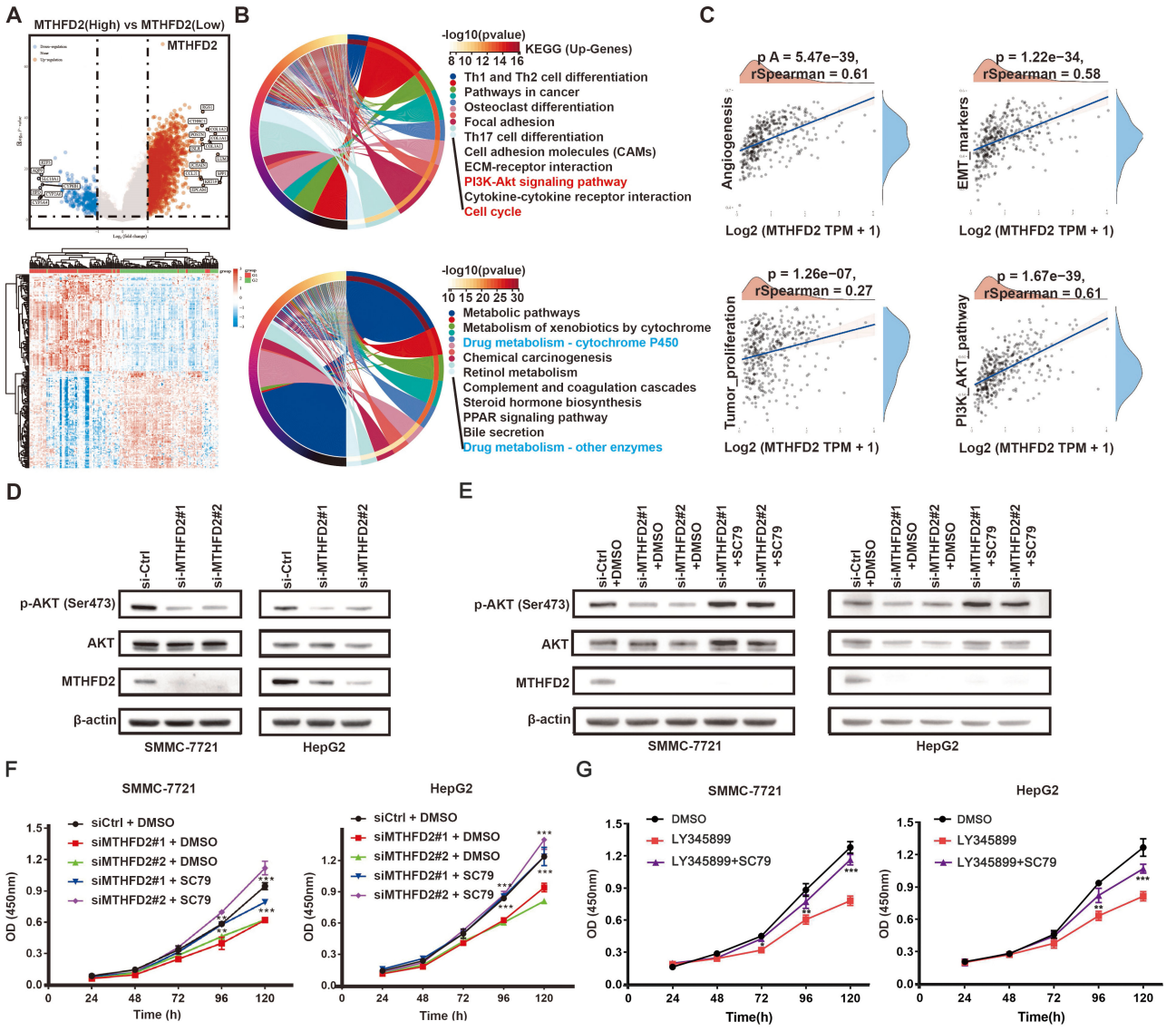

Fig. 4. MTHFD2 regulates HCC cell proliferation via PI3K/AKT signaling pathway. (A) Volcano plots of the DEGs between MTHFD2-high and MTHFD2-low groups. (B) Results of KEGG enrichment analysis of DEGs between high-expression and low-expression groups of MTHFD2. (C) Correlation analysis between MTHFD2 and signal pathways. (D,E) Protein levels of p-AKT, AKT, and MTHFD2 were analyzed using Western blotting in cells transfected with MTHFD2 siRNA, as well as cells treated with or without the AKT pathway activator SC79 (15 μM, 24 h). (F) CCK-8 assay was used to assess cell proliferation in cells transfected with MTHFD2 siRNAs, with or without the AKT activator SC79 (15 μM, 24 h). (G) CCK-8 assay was used to assess cell proliferation in cells incubated with LY345899 (50 μM, 72 h), with or without SC79 (15 μM, 24 h). Experiments were performed three times independently and the data were represented as the means ± SD. $^{**}p < 0.01$, $^{***}p < 0.001$.

significantly affects intracellular oxidative phosphorylation, purine metabolism, and serine/glycine metabolism in breast cancer cells [29]. Additionally, MTHFD2 silencing could trigger apoptosis by altering NADPH/NADP levels in cancer cells [30]. Driven by our initial observation that MTHFD2 is associated with poor HCC prognosis, we investigated the role of MTHFD2 in HCC development. We noted that knockdown of MTHFD2 led to reduced cell proliferation, suggesting the importance of this enzyme in stimulating HCC growth and malignancy. Using bioinformatic analyses, we found that MTHFD2 may mediate HCC development through PI3K/AKT signaling. Subsequent examination of p-AKT displayed a decrease in abundance in response to MTHFD2 knockdown. In addition, the AKT agonist SC79 rescued the suppressive impact of MTHFD2 siRNAs on cellular growth. Taken together, our findings demonstrate that MTHFD2 facilitates HCC cell proliferation through enhanced PI3K/AKT signaling pathway activity.

Emerging evidence has indicated that mitochondrial enzymes in folate metabolism play critical roles in tumor chemosensitivity. For example, SHMT2-mediated com-

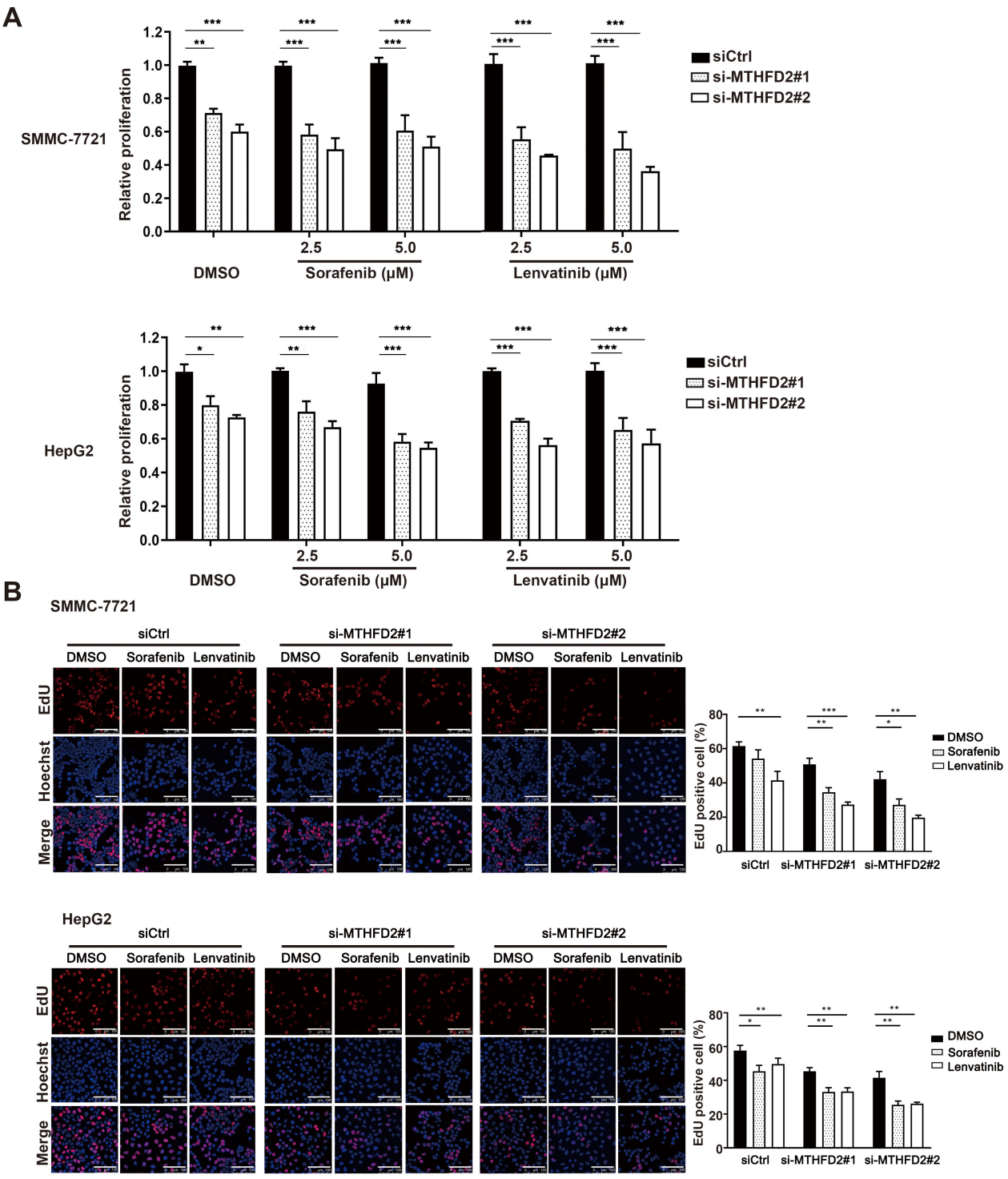

Fig. 5. Knockdown of MTHFD2 sensitized HCC cells to sorafenib and lenvatinib treatment. (A) Proliferation of SMMC-7721 and HepG2 cells treated with MTHFD2 siRNAs in the presence of control, different concentrations of sorafenib or lenvatinib. (B) DNA synthesis in SMMC-7721 and HepG2 cells treated with MTHFD2 siRNAs in the presence of DMSO, sorafenib, or lenvatinib. Photographs were taken under an optical microscope with a magnification of 400×. Experiments were performed three times independently and the data were represented as the means ± SD. *$p < 0.05$, **$p < 0.01$, ***$p < 0.001$.

partmentalization of folate metabolism drives 5-FU resistance in colorectal cancer [31]. Further, knockdown of the circular RNA circ-MTHFD1L combined with olaparib sensitizes the pancreatic cancer cells to gemcitabine [32]. Also, downregulation of MTHFD2 restored gefitinib sensitivity and diminished stem-like characteristics in drug-resistant lung cancer cells [33]. In this study, we demonstrated that downregulation of MTHFD2 rendered HCC

cells more sensitive to sorafenib and lenvatinib, suggesting a novel strategy for improving HCC chemosensitivity. However, the molecular mechanisms underlying this MTHFD2-dependent effect on chemoresistance in HCC require further exploration.

5. Conclusions

In summary, elevated expression of MTHFD2 mRNA and protein is commonly found in HCC, and overexpression of MTHFD2 is associated with aggressive clinical features in this tumor type. MTHFD2 expression, when combined with heightened Ki-67 expression, serves as a refined prognostic indicator for HCC patients. Furthermore, we demonstrated that MTHFD2 plays a critical role in HCC cell proliferation and chemosensitivity. Collectively, our findings provide new insights into the development of HCC, and the potential for MTHFD2 as a promising target for effective treatment of HCC.

Abbreviations

HCC, hepatocellular carcinoma; MTHFD2, methylenetetrahydrofolate dehydrogenase 2; FOCM, folate-mediated one-carbon metabolism; NADPH, nicotinamide adenine dinucleotide phosphate hydrogen; siRNA, small interfering RNA; LI, labeling index; KEGG, kyoto encyclopedia of genes and genomes; GO, gene ontology; GEO, gene expression omnibus; GSEA, gene set enrichment analysis; DEG, differentially expressed genes; TCGA, the cancer genome atlas; TYMS, thymidylate synthetase; ALDH1L1, aldehyde dehydrogenase 1 family member L1; NES, normalized enrichment score; SHMT2, serine hydroxymethyltransferase 2; MTHFD1L, methylenetetrahydrofolate dehydrogenase 1 like.

Availability of Data and Materials

The datasets used and/or analyzed during the current study are available from the corresponding author on reasonable request.

Author Contributions

All authors contributed to the study conception and design. The research was conceived and designed by HM and FW. JW performed the majority of the experiments, while ZY was responsible for bioinformatics analysis and the design of figures. YJ, TL and YW analyzed data and collected clinical data. ZL and GZ contributed to analysis and interpretation of data. All authors contributed to editorial changes in the manuscript. All authors read and approved the final manuscript. All authors have participated sufficiently in the work and agreed to be accountable for all aspects of the work.

Ethics Approval and Consent to Participate

This study was performed in line with the principles of the Declaration of Helsinki. Approval was granted by the Ethics Committee of Zhoushan Hospital (Date.2019/No.066). Written informed consent are obtained from each subject or subject's guardian.

Acknowledgment

Not applicable.

Funding

This research was supported by the Zhejiang Provincial Natural Science Foundation of China (LGF21H160020) and the Zhoushan Science and Technology Program (2019C31076).

Conflict of Interest

The authors declare no conflict of interest.

Supplementary Material

Supplementary material associated with this article can be found, in the online version, at https://doi.org/10.31083/j.fbl2901035.

References

[1] Vogel A, Meyer T, Sapisochin G, Salem R, Saborowski A. Hepatocellular carcinoma. Lancet (London, England). 2022; 400: 1345–1362.

[2] Villanueva A. Hepatocellular Carcinoma. The New England Journal of Medicine. 2019; 380: 1450–1462.

[3] Piñero F, Dirchwolf M, Pessôa MG. Biomarkers in Hepatocellular Carcinoma: Diagnosis, Prognosis and Treatment Response Assessment. Cells. 2020; 9: 1370.

[4] Ikeda M, Kobayashi M, Tahara M, Kaneko S. Optimal management of patients with hepatocellular carcinoma treated with lenvatinib. Expert Opinion on Drug Safety. 2018; 17: 1095–1105.

[5] Hanahan D, Weinberg RA. Hallmarks of cancer: the next generation. Cell. 2011; 144: 646–674.

[6] Liberti MV, Locasale JW. The Warburg Effect: How Does it Benefit Cancer Cells? Trends in Biochemical Sciences. 2016; 41: 211–218.

[7] Eich ML, Rodriguez Pena MDC, Chandrashekar DS, Chaux A, Agarwal S, Gordetsky JB, *et al*. Expression and Role of Methylenetetrahydrofolate Dehydrogenase 1 Like (MTHFD1L) in Bladder Cancer. Translational Oncology. 2019; 12: 1416–1424.

[8] Li Z, Wang F, Liang B, Su Y, Sun S, Xia S, *et al*. Methionine metabolism in chronic liver diseases: an update on molecular mechanism and therapeutic implication. Signal Transduction and Targeted Therapy. 2020; 5: 280.

[9] Locasale JW. Serine, glycine and one-carbon units: cancer metabolism in full circle. Nature Reviews. Cancer. 2013; 13: 572–583.

[10] Quevedo-Ocampo J, Escobedo-Calvario A, Souza-Arroyo V, Miranda-Labra RU, Bucio-Ortiz L, Gutiérrez-Ruiz MC, *et al*. Folate Metabolism in Hepatocellular Carcinoma. What Do We Know So Far? Technology in Cancer Research & Treatment. 2022; 21: 15330338221144446.

[11] Fan J, Ye J, Kamphorst JJ, Shlomi T, Thompson CB, Rabinowitz JD. Quantitative flux analysis reveals folate-dependent NADPH production. Nature. 2014; 510: 298–302.

[12] Di Pietro E, Sirois J, Tremblay ML, MacKenzie RE. Mitochondrial NAD-dependent methylenetetrahydrofolate dehydrogenase-methenyltetrahydrofolate cyclohydrolase is

essential for embryonic development. Molecular and Cellular Biology. 2002; 22: 4158–4166.

[13] Nilsson R, Jain M, Madhusudhan N, Sheppard NG, Strittmatter L, Kampf C, *et al*. Metabolic enzyme expression highlights a key role for MTHFD2 and the mitochondrial folate pathway in cancer. Nature Communications. 2014; 5: 3128.

[14] Peri KG, MacKenzie RE. NAD(+)-dependent methylenetetrahydrofolate dehydrogenase-cyclohydrolase: detection of the mRNA in normal murine tissues and transcriptional regulation of the gene in cell lines. Biochimica et Biophysica Acta. 1993; 1171: 281–287.

[15] Zhangyuan G, Wang F, Zhang H, Jiang R, Tao X, Yu D, *et al*. VersicanV1 promotes proliferation and metastasis of hepatocellular carcinoma through the activation of EGFR-PI3K-AKT pathway. Oncogene. 2020; 39: 1213–1230.

[16] King KL, Hwang JJ, Chau GY, Tsay SH, Chi CW, Lee TG, *et al*. Ki-67 expression as a prognostic marker in patients with hepatocellular carcinoma. Journal of Gastroenterology and Hepatology. 1998; 13: 273–279.

[17] Wu S, Cai W, Shi Z, Ming X, Yang X, Zhou Y, *et al*. Knockdown of MTHFD2 inhibits proliferation and migration of nasopharyngeal carcinoma cells through the ERK signaling pathway. Biochemical and Biophysical Research Communications. 2022; 614: 47–55.

[18] Li G, Wu J, Li L, Jiang P. p53 deficiency induces MTHFD2 transcription to promote cell proliferation and restrain DNA damage. Proceedings of the National Academy of Sciences of the United States of America. 2021; 118: e2019822118.

[19] Zhu Z, Kiang KMY, Li N, Liu J, Zhang P, Jin L, *et al*. Folate enzyme MTHFD2 links one-carbon metabolism to unfolded protein response in glioblastoma. Cancer Letters. 2022; 549: 215903.

[20] Guzman G, Alagiozian-Angelova V, Layden-Almer JE, Layden TJ, Testa G, Benedetti E, *et al*. p53, Ki-67, and serum alpha fetoprotein as predictors of hepatocellular carcinoma recurrence in liver transplant patients. Modern Pathology. 2005; 18: 1498–1503.

[21] Takahashi K, Obeid J, Burmeister CS, Bruno DA, Kazimi MM, Yoshida A, *et al*. Intrahepatic Cholangiocarcinoma in the Liver Explant After Liver Transplantation: Histological Differentiation and Prognosis. Annals of Transplantation. 2016; 21: 208–215.

[22] de M Rêgo JF, de Medeiros RSS, Braghiroli MI, Galvão B, Neto JEB, Munhoz RR, *et al*. Expression of ERCC1, Bcl-2, Lin28a, and Ki-67 as biomarkers of response to first-line platinum-based chemotherapy in patients with high-grade extrapulmonary neuroendocrine carcinomas or small cell lung cancer. Ecancermedicalscience. 2017; 11: 767.

[23] Zhang Z, Gu W, Hu M, Zhang G, Yu F, Xu J, *et al*. Based on clinical Ki-67 expression and serum infiltrating lymphocytes related nomogram for predicting the diagnosis of glioma-grading. Frontiers in Oncology. 2022; 12: 696037.

[24] Go SI, Ko GH, Lee WS, Lee JH, Jeong SH, Lee YJ, *et al*. The Use of CD44 Variant 9 and Ki-67 Combination Can Predicts Prognosis Better Than Their Single Use in Early Gastric Cancer. Cancer Research and Treatment. 2019; 51: 1411–1419.

[25] Al-Keilani MS, Bdeir R, Elstaty RI, Alqudah MA. Expression of substance P, neurokinin 1 receptor, Ki-67 and pyruvate kinase M2 in hormone receptor negative breast cancer and evaluation of impact on overall survival. BMC Cancer. 2023; 23: 158.

[26] Menon SS, Guruvayoorappan C, Sakthivel KM, Rasmi RR. Ki-67 protein as a tumour proliferation marker. Clinica Chimica Acta; International Journal of Clinical Chemistry. 2019; 491: 39–45.

[27] Lee GY, Haverty PM, Li L, Kljavin NM, Bourgon R, Lee J, *et al*. Comparative oncogenomics identifies PSMB4 and SHMT2 as potential cancer driver genes. Cancer Research. 2014; 74: 3114–3126.

[28] Tibbetts AS, Appling DR. Compartmentalization of Mammalian folate-mediated one-carbon metabolism. Annual Review of Nutrition. 2010; 30: 57–81.

[29] Xie SY, Shi DB, Ouyang Y, Lin F, Chen XY, Jiang TC, *et al*. SHMT2 promotes tumor growth through VEGF and MAPK signaling pathway in breast cancer. American Journal of Cancer Research. 2022; 12: 3405–3421.

[30] Yang S, Wong KH, Hua P, He C, Yu H, Shao D, *et al*. ROS-responsive fluorinated polyethyleneimine vector to co-deliver shMTHFD2 and shGPX4 plasmids induces ferroptosis and apoptosis for cancer therapy. Acta Biomaterialia. 2022; 140: 492–505.

[31] Pranzini E, Pardella E, Muccillo L, Leo A, Nesi I, Santi A, *et al*. SHMT2-mediated mitochondrial serine metabolism drives 5-FU resistance by fueling nucleotide biosynthesis. Cell Reports. 2022; 40: 111233.

[32] Chen ZW, Hu JF, Wang ZW, Liao CY, Kang FP, Lin CF, *et al*. Circular RNA circ-MTHFD1L induces HR repair to promote gemcitabine resistance via the miR-615-3p/RPN6 axis in pancreatic ductal adenocarcinoma. Journal of Experimental & Clinical Cancer Research: CR. 2022; 41: 153.

[33] Nishimura T, Nakata A, Chen X, Nishi K, Meguro-Horike M, Sasaki S, *et al*. Cancer stem-like properties and gefitinib resistance are dependent on purine synthetic metabolism mediated by the mitochondrial enzyme MTHFD2. Oncogene. 2019; 38: 2464–2481.